Polarization properties of Maxwell-Gaussian laser beams

W. L. Erikson* and Surendra Singh
Department of Physics, University of Arkansas, Fayetteville, Arkansas 72701
(Received 10 December 1993)

Gaussian beam solutions of Maxwell's equations are constructed in terms of the solutions of the paraxial scalar wave equation. Explicit expressions for the field components of Hermite-Gaussian laser beams are given and their polarization and propagation characteristics are discussed. Experimental evidence for the polarization structure of Hermite-Gaussian laser beams is presented.

PACS number(s): 42.25.Ja, 42.60.Jf, 41.20.−q

I. INTRODUCTION

Laser beams are wavelike electromagnetic disturbances that have a predominant direction of propagation and a finite cross section transverse to the direction of propagation. These beams are commonly modeled by Hermite-Gaussian beams [1–3]. This is usually done within the framework of the scalar and paraxial approximations. For most applications which do not involve the polarization properties of laser beams, this framework is quite adequate. However, a scalar representation fails to describe the polarization properties of laser beams correctly. Indeed, a scalar description of finite cross-section laser beams is inconsistent with Maxwell's equations even for linearly polarized laser beams. The transverse character of the electromagnetic field, expressed by two of Maxwell's equations $\vec{\nabla}\cdot\vec{E}(\vec{r},t)=0$ and $\vec{\nabla}\cdot\vec{B}(\vec{r},t)=0$, implies that the spatial variation of the field in directions transverse to the direction of propagation is coupled to the polarization properties of the field. Thus it is well known that spatial variation of the field in transverse directions gives rise to a longitudinal field component [4–11].

The coupling of transverse spatial variation of nonplanar wave fronts to polarization was investigated in an interesting paper by Fainman and Shamir [6]. They analyzed the cross polarization in a spherical wave front from a point source. They also recorded experimentally the cross polarization of a linearly polarized fundamental Gaussian beam passing through a pin hole. Several other workers have also discussed the polarization properties of the fundamental Gaussian laser beam [7,8]. They show that the fundamental Gaussian beam will always exhibit cross polarization even without passing through a pin hole. The general problem of beamlike solutions of Maxwell's equations has also been treated by several workers [9,10] in terms of electromagnetic potentials.

In this paper we present a simpler and more direct approach based on the solutions of the paraxial wave equation. Using this approach we establish the general field (polarization) structure of paraxial beamlike solutions of Maxwell's equations. These expressions are then used to describe explicitly the polarization and propagation characteristics of the fundamental as well as higher order Hermite-Gaussian laser beams. Finally, we present an experimental confirmation of the polarization structure of Hermite-Gaussian laser beams.

We begin by summarizing the properties of the solutions of the paraxial scalar wave equation in Sec. II. We then construct paraxial beam solutions of Maxwell's equations from the solutions of the paraxial scalar wave equation in Sec. III. Polarization properties of Hermite-Gaussian laser beams are then discussed in Sec. IV. Finally, in Sec. V, we present an experimental confirmation of the polarization properties Hermite-Gaussain laser beams.

II. THE SCALAR WAVE EQUATION

The scalar wave function $\psi(\vec{r},t)$ in free space satisfies the source free wave equation

$$\left[\nabla^2-\frac{1}{c^2}\frac{\partial^2}{\partial t^2}\right]\psi(\vec{r},t)=0, \tag{1}$$

where ∇^2 is the three dimensional Laplacian operator and c is the wave speed. For electromagnetic waves c is the speed of light. For quasimonochromatic waves of angular frequency ω, propagating predominantly in the z direction, the wave amplitude has the form

$$\psi(\vec{r},t)=\psi(\vec{r})e^{i(kz-\omega t)}, \tag{2}$$

where $\psi(\vec{r})$ describes the variation of the wave amplitude in transverse directions (x-y plane). Propagation constant k is related to the wavelength λ and the angular frequency ω of the wave by

$$k=\frac{\omega}{c}=\frac{2\pi}{\lambda}. \tag{3}$$

For paraxial beams, the energy is concentrated near the axis of the beam and the transverse profile of the beam, as described by $\psi(\vec{r})$, varies little with z over propagation

*Present address: U.S. Air Force Academy, Colorado Springs, CO 80840.

distances of the order of a few wavelengths. For smooth transverse profile $\psi(\vec{r})$, the slow variation of beam profile during propagation implies that the following inequalities hold:

$$\frac{1}{k}\left|\frac{\partial\psi(\vec{r})}{\partial z}\right| = \frac{\lambda}{2\pi}\left|\frac{\partial\psi(\vec{r})}{\partial z}\right| \ll |\psi(\vec{r})|, \tag{4}$$

$$\frac{1}{k}\left|\frac{\partial}{\partial z}\left(\frac{\partial\psi(\vec{r})}{\partial z}\right)\right| = \frac{\lambda}{2\pi}\left|\frac{\partial}{\partial z}\left(\frac{\partial\psi(\vec{r})}{\partial z}\right)\right| \ll \left|\frac{\partial\psi(\vec{r})}{\partial z}\right|. \tag{5}$$

Substituting Eq. (2) into Eq. (1) and using Eqs. (3)-(5) we find that $\psi(\vec{r})$ satisfies the paraxial wave equation

$$\frac{\partial^2\psi(\vec{r})}{\partial x^2} + \frac{\partial^2\psi(\vec{r})}{\partial y^2} + 2ik\frac{\partial\psi}{\partial z} = 0. \tag{6}$$

This equation relates the variation of the beam profile $\psi(\vec{r})$ in the transverse and longitudinal directions. Solutions of this equation in free space are labeled by two indices. The well-known solutions with rectangular symmetry (separable in Cartesian coordinates) are the Hermite-Gaussian solutions given by [1–3]

$$\psi_{mn}(\vec{r}) = \sqrt{\frac{2}{\pi w^2(z)}}\, H_m(\sqrt{2}x/w(z))H_n(\sqrt{2}y/w(z)) \times e^{-i(m+n+1)\theta(z)+ik\rho^2/2q(z)}. \tag{7}$$

Here $H_m(x)$ is a Hermite polynomial of degree m and argument x and $\rho = \sqrt{x^2+y^2}$ is the radial distance from the beam axis. The phase angle $\theta(z)$ and the complex beam parameter $q(z)$ are given by

$$\theta(z) = \tan^{-1}(z/z_0), \tag{8}$$

$$\frac{1}{q(z)} = \frac{1}{R(z)} + i\frac{2}{kw^2(z)}, \tag{9}$$

where $w(z)$ is the beam spot size in the plane that intersects the beam axis at z and $R(z)$ is the radius of curvature of the phase front that intersects the beam axis at point z. The dependence of $w(z)$ and $R(z)$ on z is given by

$$w(z) = w_0\sqrt{1+(z/z_0)^2}, \tag{10}$$

$$R(z) = z + z_0^2/z, \tag{11}$$

where w_0 is the minimum beam spot size which is attained in the $z=0$ plane. Parameter z_0 is half the confocal parameter of the beam. In terms of the minimum spot size w_0 and the propagation constant k it is given by

$$z_0 = \frac{kw_0^2}{2}. \tag{12}$$

The paraxial beam solutions given by Eq. (7) are characterized by the beam spot size $w(z)$ and the phase front radius of curvature $R(z)$. They maintain their form during propagation. Spot size $w(z)$ sets the length scale over which beam profile changes significantly in the transverse directions for a fixed value of z and z_0 sets the length scale over which beam profile changes significantly as the wave propagates.

Scalar wave equation (6) admits other paraxial beam solutions with other symmetries also. For example, in the presence of cylindrical symmetry about the z axis, Eq. (6) admits Laguerre-Gaussian beam solutions [1–3]. There are also the so called Bessel beam or the nondiffracting beam solutions [3]. In practice, symmetries other than the rectangular symmetry are difficult to realize. The presence of Brewster surfaces and other nonsymmetric optical elements in laser resonators naturally leads to rectangular symmetry. For this reason we consider only the Hermite-Gaussian solutions explicitly in this paper. From the general results derived in the paper, solutions reflecting other symmetries can be constructed.

III. PARAXIAL BEAM SOLUTIONS OF MAXWELL'S EQUATIONS

We now proceed to determine the form of paraxial solutions of Maxwell's equations. For quasimonochromatic waves propagating in the z direction we write the electric and the magnetic fields of the wave as

$$\vec{E}(\vec{r},t) = \vec{E}(\vec{r})e^{i(kz-\omega t)} \equiv [\hat{e}_1E_1(\vec{r}) + \hat{e}_2E_2(\vec{r}) + \hat{e}_3E_3(\vec{r})]e^{i(kz-\omega t)}, \tag{13}$$

$$\vec{B}(\vec{r},t) = \vec{B}(\vec{r})e^{i(kz-\omega t)} \equiv [\hat{e}_1B_1(\vec{r}) + \hat{e}_2B_2(\vec{r}) + \hat{e}_3B_3(\vec{r})]e^{i(kz-\omega t)}, \tag{14}$$

where $\vec{E}(\vec{r})$ and $\vec{B}(\vec{r})$ describe the transverse spatial profile of the beam and $\hat{e}_1$, $\hat{e}_2$, and $\hat{e}_3$ are three unit vectors along the x, y, and z axes, respectively. For the fields in Eq. (13) and (14), Maxwell's equations in free space become

$$ik\vec{E}_3(\vec{r}) + \vec{\nabla}\cdot\vec{E}(\vec{r}) = 0, \tag{15}$$

$$ik\vec{B}_3(\vec{r}) + \vec{\nabla}\cdot\vec{B}(\vec{r}) = 0, \tag{16}$$

$$ik\hat{e}_3\times\vec{E}(\vec{r}) + \vec{\nabla}\times\vec{E}(\vec{r}) = ikc\vec{B}(\vec{r}), \tag{17}$$

$$ik\hat{e}_3\times\vec{B}(\vec{r}) + \vec{\nabla}\times\vec{B}(\vec{r}) = -i\frac{k}{c}\vec{E}(\vec{r}). \tag{18}$$

By eliminating $\vec{E}(\vec{r})$ or $\vec{B}(\vec{r})$ from these equations, we see that each Cartesian component of the field vectors satisfies the scalar wave equation. For paraxial beam solutions, each field component satisfies the paraxial wave equation (6) and has the form of Eq. (7). However, various field components cannot be chosen arbitrarily. They are coupled via Eqs. (15)–(18). We now establish the general field structure of paraxial electromagnetic beams.

In the paraxial approximation of Eqs. (4) and (5), Eqs. (15) and (16) allow us to express the longitudinal field components $E_3(\vec{r})$ and $B_3(\vec{r})$ in terms of the transverse field components as

$$E_3(\vec{r}) = \frac{i}{k}\left(\frac{\partial E_1}{\partial x} + \frac{\partial E_2}{\partial y}\right), \tag{19}$$

$$B_3(\vec{r}) = \frac{i}{k}\left(\frac{\partial B_1}{\partial x} + \frac{\partial B_2}{\partial y}\right). \tag{20}$$

Next, substituting Eqs. (19) and (20) into Eq. (17) and

using the inequalities (4) and (5), we can express the magnetic field components in terms of the electric field components

$$c\vec{B}_1(\vec{r}) = -\vec{E}_2(\vec{r}) + \frac{1}{2k^2}\left(\frac{\partial^2\vec{E}_2(\vec{r})}{\partial y^2} - \frac{\partial^2\vec{E}_2(\vec{r})}{\partial x^2}\right) + \frac{1}{k^2}\frac{\partial^2\vec{E}_1(\vec{r})}{\partial x\partial y}, \tag{21}$$

$$c\vec{B}_2(\vec{r}) = \vec{E}_1(\vec{r}) + \frac{1}{2k^2}\left(\frac{\partial^2\vec{E}_1(\vec{r})}{\partial y^2} - \frac{\partial^2\vec{E}_1(\vec{r})}{\partial x^2}\right) - \frac{1}{k^2}\frac{\partial^2\vec{E}_2(\vec{r})}{\partial x\partial y}, \tag{22}$$

$$c\vec{B}_3(\vec{r}) = -\frac{i}{k}\left(\frac{\partial\vec{E}_2(\vec{r})}{\partial x} - \frac{\partial\vec{E}_1(\vec{r})}{\partial y}\right). \tag{23}$$

Similarly, using Eqs. (19) and (20) in Eq. (18), we can express the electric field components in terms of the magnetic field components

$$\vec{E}_1(\vec{r}) = c\left[\vec{B}_2(\vec{r}) + \frac{1}{2k^2}\left(\frac{\partial^2\vec{B}_2(\vec{r})}{\partial x^2} - \frac{\partial^2\vec{B}_2(\vec{r})}{\partial y^2}\right) - \frac{1}{k^2}\frac{\partial^2\vec{B}_1(\vec{r})}{\partial x\partial y}\right], \tag{24}$$

$$\vec{E}_2(\vec{r}) = c\left[-\vec{B}_1(\vec{r}) + \frac{1}{2k^2}\left(\frac{\partial^2\vec{B}_1(\vec{r})}{\partial x^2} - \frac{\partial^2\vec{B}_1(\vec{r})}{\partial y^2}\right) + \frac{1}{k^2}\frac{\partial^2\vec{B}_2(\vec{r})}{\partial x\partial y}\right], \tag{25}$$

$$\vec{E}_3(\vec{r}) = i\frac{c}{k}\left(\frac{\partial\vec{B}_2(\vec{r})}{\partial x} - \frac{\partial\vec{B}_1(\vec{r})}{\partial y}\right) \tag{26}$$

An inspection of these equations shows that the electric and magnetic field components can be expressed in terms of two independent solutions $f(\vec{r})$ and $g(\vec{r})$ of the paraxial wave equation. Then the electric and the magnetic field components can be written as

$$\vec{E}_1(\vec{r}) = f(\vec{r}) + \frac{1}{4k^2}\left(\frac{\partial^2 f(\vec{r})}{\partial x^2} - \frac{\partial^2 f(\vec{r})}{\partial y^2}\right) + \frac{1}{2k^2}\frac{\partial^2 g(\vec{r})}{\partial x\partial y}, \tag{27}$$

$$\vec{E}_2(\vec{r}) = g(\vec{r}) - \frac{1}{4k^2}\left(\frac{\partial^2 g(\vec{r})}{\partial x^2} - \frac{\partial^2 g(\vec{r})}{\partial y^2}\right) + \frac{1}{2k^2}\frac{\partial^2 f(\vec{r})}{\partial x\partial y}, \tag{28}$$

$$\vec{E}_3(\vec{r}) = \frac{i}{k}\left(\frac{\partial f(\vec{r})}{\partial x} + \frac{\partial g(\vec{r})}{\partial y}\right), \tag{29}$$

$$c\vec{B}_1(\vec{r}) = -g(\vec{r}) + \frac{1}{4k^2}\left(\frac{\partial^2 g(\vec{r})}{\partial y^2} - \frac{\partial^2 g(\vec{r})}{\partial x^2}\right) + \frac{1}{2k^2}\frac{\partial^2 f(\vec{r})}{\partial x\partial y}, \tag{30}$$

$$c\vec{B}_2(\vec{r}) = f(\vec{r}) + \frac{1}{4k^2}\left(\frac{\partial^2 f(\vec{r})}{\partial y^2} - \frac{\partial^2 f(\vec{r})}{\partial x^2}\right) - \frac{1}{2k^2}\frac{\partial^2 g(\vec{r})}{\partial x\partial y}, \tag{31}$$

$$c\vec{B}_3(\vec{r}) = -\frac{i}{k}\left(\frac{\partial g(\vec{r})}{\partial x} - \frac{\partial f(\vec{r})}{\partial y}\right). \tag{32}$$

It is easily checked that Eqs. (27)–(32) satisfy the paraxial Maxwell's equations (19)–(26) up to terms of order $(k\ell)^{-2}$, where ℓ is some characteristic length associated with the transverse variation of the beam profile.

For Hermite-Gaussian solutions given by Eq. (7), the length ℓ is of the order of the beam spot size w for variations in the transverse dimensions and for variations in the longitudinal direction it is of the order of z_0. Then, in order of magnitude, the terms involving the first and the second order derivatives in Eqs. (27)–(32) are of order $f/(kw), g/(kw)$ and $f/(kw)^2, g/(kw)^2$. If $kw \gg 1$ (or $w \gg \lambda$), that is, if the beam is many wavelengths wide, these terms are small and the solutions have the form of a perturbative series in powers of the small parameter $(kw)^{-1} \approx \lambda/(2\pi w)$. Equations (27)–(32) are similar to the results derived by other workers [9,10], but the physical significance of $f(\vec{r})$ and $g(\vec{r})$ here is different. In the next section we construct explicit examples of these solutions for Hermite-Gaussian laser beams.

IV. HERMITE GAUSSIAN ELECTROMAGNETIC BEAMS

Electromagnetic beams generated by most lasers have rectangular symmetry. We therefore consider Hermite-Gaussian electromagnetic beams to describe laser beams and discuss their polarization and propagation characteristics.

From Eqs. (27)–(32) we see that finite cross section electromagnetic waves must have a longitudinal field component. In this sense pure transverse electromagnetic beams do not exist. However, since the longitudinal field component is smaller by a factor $1/kw$ compared to the dominant transverse field component, it is still possible to have electromagnetic beams that have dominant transverse polarization. We now examine the forms of linearly and circularly polarized electromagnetic beams.

A. Linearly polarized electromagnetic beams

Without loss of generality, we take the direction of dominant polarization to be the x direction. Then, by choosing $f(\vec{r}) = \psi_{mn}(\vec{r})$ and $g(\vec{r}) = 0$, we find that Eqs. (27)–(29) for the electric field components take the form

$$E_1^{(mn)}(\vec{r}) = A_{mn}\psi_{mn}(\vec{r}), \tag{33}$$

$$E_2^{(mn)}(\vec{r}) = \left(\frac{A_{mn}}{2k^2}\right)\frac{\partial^2\psi_{mn}(\vec{r})}{\partial x\partial y}, \tag{34}$$

$$E_3^{(mn)}(\vec{r}) = \left(\frac{iA_{mn}}{k}\right)\frac{\partial\psi_{mn}(\vec{r})}{\partial x}, \tag{35}$$

where A_{mn} is a constant related to the power carried by the wave and $\psi_{mn}(\vec{r})$ represents a Hermite-Gaussian beam solution of the paraxial scalar wave equation given by Eq. (7). Magnetic field components corresponding to Eqs. (33)–(35) are obtained by the relations $cB_1 = E_2$, $cB_2 = -E_1$, and $cB_3 = (i/k)\partial E_1/\partial y$. In writing Eq. (33) we have dropped terms involving second order derivatives of $\psi_{mn}(\vec{r})$ since, according to Eqs. (4) and (5), they are smaller by the factor $1/(kw)^2$ compared to the leading term. Similarly, for the longitudinal and the cross-polarization fields we have kept only the leading terms.

Using the properties of Hermite polynomials [12] we arrive at the following expressions for the fields:

$$E_1^{(mn)}(\vec{r}) = A_{mn}\psi_{mn}(\vec{r}), \tag{36}$$

$$E_2^{(mn)}(\vec{r}) = \frac{A_{mn}}{4(kw_0)^2}[4mn\psi_{m-1,n-1}(\vec{r}) - 2m\psi_{m-1,n+1}(\vec{r}) - 2n\psi_{m+1,n-1}(\vec{r}) + \psi_{m+1,n+1}(\vec{r})], \tag{37}$$

$$E_3^{(mn)}(\vec{r}) = \frac{iA_{mn}}{\sqrt{2}kw_0}[2m\psi_{m-1,n}(\vec{r}) - \psi_{m+1,n}(\vec{r})]. \tag{38}$$

Similar equations hold for the components of the magnetic field. These equations explicitly indicate the relative magnitudes of various field components. A more quantitative measure of the relative strengths of field components is obtained by comparing the powers associated with different field components. The total power P_0 associated with the beam is given by

$$P_0 = \frac{1}{2}\epsilon_0 c\,\mathrm{Re}\int\int \vec{E}(\vec{r})\cdot\vec{E}^*(\vec{r})dxdy = \frac{1}{2}\epsilon_0 c\,|A_{mn}|^2\,2^{m+n}m!n!\,. \tag{39}$$

This equation determines the constant A_{mn} in terms of the total beam power P_0. The power P_i associated with different field components is then given by

$$P_1 = \frac{P_0}{2}, \tag{40}$$

$$P_2 = \frac{P_0}{2}\frac{(2m+1)(2n+1)}{4(kw_0)^4}, \tag{41}$$

$$P_3 = \frac{P_0}{2}\frac{(2m+1)}{(kw_0)^2}. \tag{42}$$

It follows from these equations that the power associated with different field components is independent of z. This means the power associated with each field component remains constant during propagation. Equations (40)–(42) together with Eqs. (37) and (38) also show that an electromagnetic beam predominantly polarized in the x direction has a small cross-polarization component in the y direction in addition to a small longitudinal component. The longitudinal field component is smaller by a factor of $1/kw_0$ and the cross-polarization field component is smaller by a factor of $1/(kw_0)^2$ compared to the dominant polarization component. From these considerations it is clear that, in general, for finite cross-section beams (kw_0 finite), both the cross-polarization and longitudinal field components must be kept for consistency with Maxwell's equations. In the special case $m = 0 = n$, the expressions for the fields given in Eqs. (36)–(38) reduce to the results derived in Refs. [5–7] for the fundamental Gaussian beam.

The presence of longitudinal field component $E_3^{(mn)}(\vec{r})$ is also required for a correct description of energy flow in the beam. Energy flow in a beam is described in terms of rays, which are geometric curves such that the tangent to a ray at a given point indicates the direction of the Poynting vector (local energy flow). For Hermite-Gaussian electromagnetic beams, rays should converge as they approach the beam waist (focal region) and diverge as they leave the focal region. When the longitudinal field component is kept, the Poynting vector has this property. The Poynting vector averaged over an optical cycle is

$$\vec{S}(\vec{r}) = \frac{1}{2}\epsilon_0 c^2\,\mathrm{Re}[\vec{E}(\vec{r})\times\vec{B}^*(\vec{r})]. \tag{43}$$

Using the fields given by Eqs. (36)–(38) and certain recursion relations for Hermite polynomials [12], we find that the Poynting vector for a Hermite-Gaussian beam can be written as

$$\vec{S} = \frac{1}{2}\epsilon_0 c\,|A_{mn}|^2\,|\psi_{mn}(\vec{r})|^2\left[\hat{e}_1\frac{x}{R(z)} + \hat{e}_2\frac{y}{R(z)} + \hat{e}_3\right]. \tag{44}$$

The quantity outside the square brackets is simply the beam intensity ($\mathrm{W/m^2}$). The vector inside the square brackets denotes the direction of energy flow. If we recall that the radius of curvature $R(z)$ is negative for a converging wave and positive for a diverging wave [1–3], it follows from Eq. (44) that for a beam approaching the focal region, energy flow occurs toward the z axis and for a beam leaving the focal region energy flow occurs away from the z axis (see Fig. 1). If the longitudinal components of the fields are ignored, energy flow occurs only in the z direction. Such a beam is not only inconsistent with Maxwell's equations, but also fails to account for the focusing properties of laser beams correctly. From Eq. (44) we find the equation for the family of rays is

$$\rho = \rho_0\sqrt{(z/z_0)^2 + 1}, \tag{45}$$

where $\rho = \sqrt{x^2+y^2}$ and ρ_0 is the distance of the ray from the beam axis at the beam waist $z = 0$. Figure 1 shows the direction of the Poynting vector $\vec{S}$, the asso-

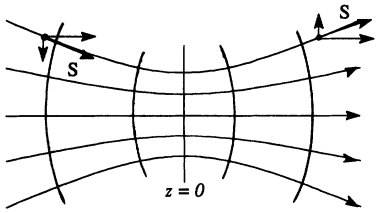

FIG. 1. Energy flow in the focal region for a Gaussian beam propagating to the right. Directed line segments represent ray trajectories and curves orthogonal to them represent wavefronts.

ciated ray trajectories, and the wave fronts in the focal region for a wave propagating to the right.

The cross-polarization component $E_2^{(mn)}(\vec{r})$ is even smaller than the longitudinal field component. If the polarization properties of the wave are not of interest, the cross-polarization component may be ignored. However, for a correct description of the polarization properties, this component must be kept. For example, if the beam passes through a linear polarizer whose transmission axis is crossed with respect to the dominant direction of polarization, the cross-polarization component is the dominant component in the transmitted beam.

It is interesting to compare the distributions of fields in a plane transverse to the direction of propagation. In general, the transverse distributions of fields evolve during propagation. It is interesting to note that this evolution does not involve a change in the energies associated with different field components. This follows from Eqs. (40)–(42), which show that the power associated with each field component remains constant (independent of z) during propagation. Expressions (37) and (38) for the cross-polarization and the longitudinal components are complicated in general. In the far zone $z \gg z_0$; however, simple expressions can be derived. In this limit, the fields for Hermite-Gaussian beams take the form

$$E_1^{(mn)}(\vec{r}) = A_{mn}\psi_{mn}(\vec{r}), \tag{46}$$

$$E_2^{(mn)}(\vec{r}) = \frac{1}{(kw_0)^2}\left(\frac{2xy}{w^2(z)}\right) A_{mn}\psi_{mn}(\vec{r}), \tag{47}$$

$$E_3^{(mn)}(\vec{r}) = \frac{2i}{kw_0}\left(\frac{x}{w(z)}\right) A_{mn}\psi_{mn}(\vec{r}), \tag{48}$$

where $\psi_{mn}(\vec{r})$ is given by Eq. (7). These expressions for the field components, with the help of Eq. (39), lead to the following transverse intensity distributions for the fields:

$$I_1^{(mn)}(\vec{r}) = \left[\frac{P_0}{2^{m+n}m!n!\pi w^2(z)}\right] \times H_m^2(X)H_n^2(Y)e^{-(X^2+Y^2)}, \tag{49}$$

$$I_2^{(mn)}(\vec{r}) = \left[\frac{1}{(kw_0)^4}\right] X^2Y^2 I_1^{(mn)}(\vec{r}), \tag{50}$$

$$I_3^{(mn)}(\vec{r}) = \left[\frac{2}{(kw_0)^2}\right] X^2 I_1^{(mn)}(\vec{r}). \tag{51}$$

Here we have used the abbreviated notation, $X = \sqrt{2}\ x/w(z)$ and $Y = \sqrt{2}\ y/w(z)$. Figures 2–4 show these distributions for some lower order electromagnetic beams. For the fundamental Gaussian beam ($m = 0 = n$) polarized along the x axis, these equations lead to

$$I_1^{(00)}(\vec{r}) = \left[\frac{P_0}{\pi w^2(z)}\right] e^{-(X^2+Y^2)}, \tag{52}$$

$$I_2^{(00)}(\vec{r}) = \frac{1}{(kw_0)^4}\left[\frac{P_0}{\pi w^2(z)}\right] X^2Y^2\, e^{-(X^2+Y^2)}, \tag{53}$$

$$I_3^{(00)}(\vec{r}) = \frac{2}{(kw_0)^2}\left[\frac{P_0}{\pi w^2(z)}\right] X^2 e^{-(X^2+Y^2)}. \tag{54}$$

These intensity distributions for the fundamental beam, although derived from the asymptotic expressions (49)–(51), are valid for all values of z. It follows that the intensity distributions for the fundamental beam are form invariant as the beam propagates. These distributions for the fundamental beam agree with the results of Refs. [7,8] and are shown in Fig. 2. For higher order beams, the intensity distribution associated with the dominant polarization component remains form invariant. However, in general, the intensity distributions associated

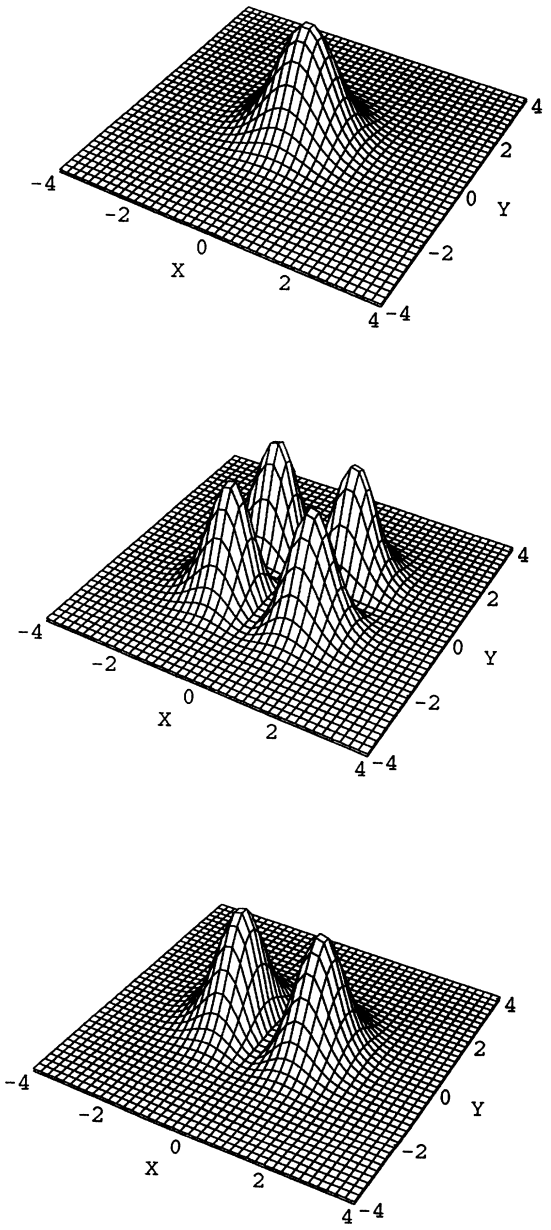

FIG. 2. Transverse intensity profiles for a Gaussian TEM_{00} wave polarized in the x direction and propagataing in the z direction. The profiles are (top to bottom) for the dominant polarization (x component), the cross-polarization component (y component), and the longitudinal component (z component). $X = \sqrt{2}\ x/w(z)$ and $Y = \sqrt{2}y\ /w(z)$ are the scaled coordinates, where $w(z)$ is the spot size at location z. Vertical axes in the three profiles are not to scale.

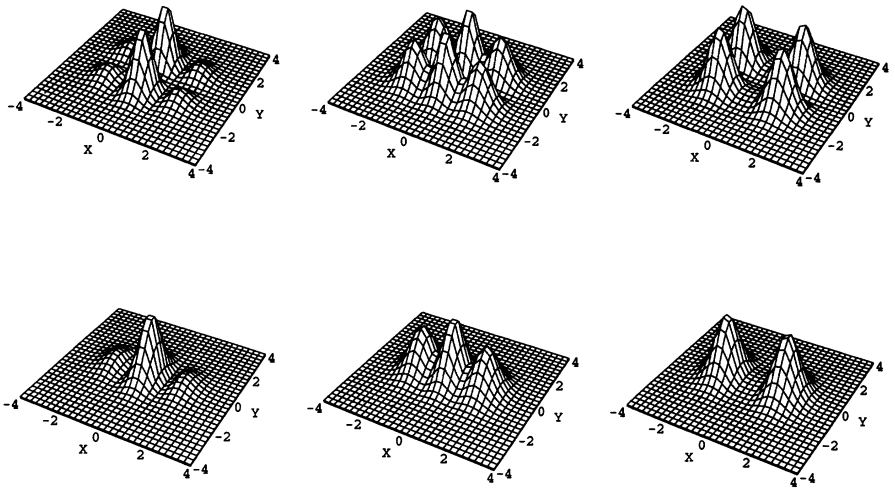

FIG. 3. Evolution of the intensity profiles associated with the cross-polarization (top profiles) and the longitudinal field (bottom profiles) components for a TEM_{10} beam. These profiles are shown for (left to right) for $z = 0$, $z = z_0$, and $z = 5z_0$. $X = \sqrt{2}\, x/w(z)$ and $Y = \sqrt{2}\, y/w(z)$ are the scaled coordinates. Vertical axes in the two rows are not to scale.

with the cross-polarization and the longitudinal components evolve during propagation. For some low order modes, the intensity distributions valid for all values of z are given below. For a TEM_{10} ($m = 1$ and $n = 0$) beam polarized along the x axis we have

$$I_1^{(10)}(\vec{r}) = \left[\frac{2P_0}{\pi w^2(z)}\right] X^2\, e^{-(X^2+Y^2)}, \tag{55}$$

$$I_2^{(10)}(\vec{r}) = \frac{1}{(kw_0)^4}\left[\frac{2P_0}{\pi w^2(z)}\right] \times Y^2\left[(1-X^2)^2\cos^2\theta + X^4\sin^2\theta\right] \times e^{-(X^2+Y^2)}, \tag{56}$$

$$I_3^{(10)}(\vec{r}) = \frac{2}{(kw_0)^2}\left[\frac{2P_0}{\pi w^2(z)}\right] \times Y^2\left[(1-X^2)^2\cos^2\theta + X^4\sin^2\theta\right] \times e^{-(X^2+Y^2)}. \tag{57}$$

For a TEM_{01} ($m = 0$, $n = 1$) beam polarized in the x direction we obtain

$$I_1^{(01)}(\vec{r}) = \left[\frac{2P_0}{\pi w^2(z)}\right] Y^2\, e^{-(X^2+Y^2)}, \tag{58}$$

$$I_2^{(01)}(\vec{r}) = \frac{1}{(kw_0)^4}\left[\frac{2P_0}{\pi w^2(z)}\right] \times X^2\left[(1-Y^2)^2\cos^2\theta + Y^4\sin^2\theta\right] \times e^{-(X^2+Y^2)}, \tag{59}$$

$$I_3^{(01)}(\vec{r}) = \frac{2}{(kw_0)^2}\left[\frac{2P_0}{\pi w^2(z)}\right] X^2Y^2\, e^{-(X^2+Y^2)}. \tag{60}$$

Finally, for a TEM_{11} ($m = 1 = n$) beam we find

$$I_1^{(11)}(\vec{r}) = \left[\frac{4P_0}{\pi w^2(z)}\right] X^2Y^2\, e^{-(X^2+Y^2)}, \tag{61}$$

$$I_2^{(11)}(\vec{r}) = \frac{1}{(kw_0)^4}\left[\frac{4P_0}{\pi w^2(z)}\right] \times \left[(1-X^2)^2\cos^2\theta + X^4\sin^2\theta\right] \times \left[(1-Y^2)^2\cos^2\theta + Y^4\sin^2\theta\right] e^{-(X^2+Y^2)}, \tag{62}$$

$$I_3^{(11)}(\vec{r}) = \frac{2}{(kw_0)^2}\left[\frac{4P_0}{\pi w^2(z)}\right] \times Y^2\left[(1-X^2)^2\cos^2\theta + X^4\sin^2\theta\right] \times e^{-(X^2+Y^2)}. \tag{63}$$

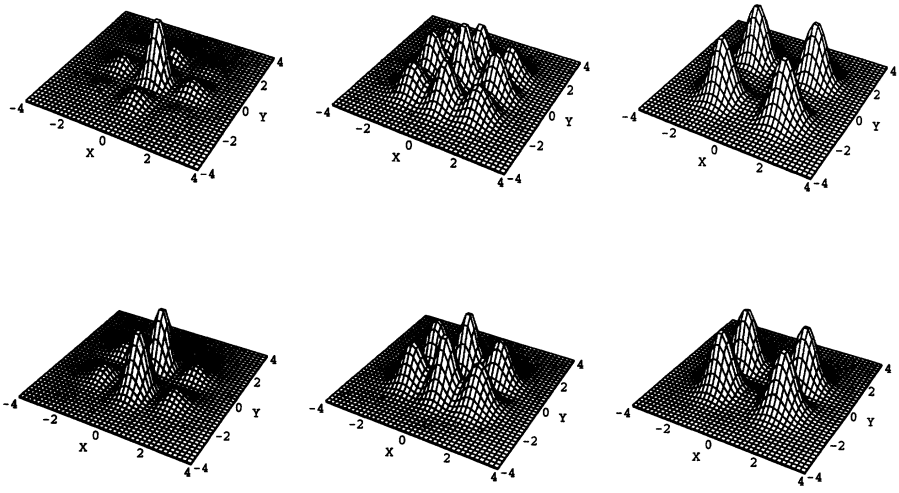

FIG. 4. Evolution of the intensity profiles associated with the cross-polarization (top profiles) and the longitudinal field (bottom profiles) components for a TEM_{11} beam. The profiles are shown (left to right) for $z = 0$, $z = z_0$, and $z = 5z_0$. $X = \sqrt{2}\, x/w(z)$ and $Y = \sqrt{2}\, y/w(z)$ are the scaled coordinates. Vertical axes in the two rows are not to scale.

Phase angle $\theta = \tan^{-1}(z/z_0)$ was introduced in Eq. (8). In the far zone $z \gg z_0$, the phase angle $\theta \to \pi/2$ and we recover the distributions given by Eqs. (49)–(51). For both TEM_{10} and TEM_{01} beams, the dominant polarization component has two lobes and its form stays constant as the beam propagates. The longitudinal component for TEM_{01} has four lobes and its form also remains constant as the beam propagates. Intensity distributions for the cross-polarization and the longitudinal components for TEM_{10} and TEM_{11} modes evolve as the beams propagate. These are shown in Figs. 3 and 4. In the far zone $z \gg z_0$, the forms of I_2 and I_3 stabilize. In this zone the cross-polarization component has a four-lobe structure. This is a general property of the cross-polarization component in the far zone, independent of the beam indices. This can be seen from Eq. (50), which shows that I_2 must vanish along the lines $x = 0$ and $y = 0$. The exact location and the detailed structure of these lobes may depend on the mode indices. Note that the intensity distribution $I_2^{(mn)}(\vec{r})$ for the cross-polarization component is what will be seen at the output of a crossed linear polarizer. Unlike the cross-polarization component, the intensity distribution for the longitudinal component does depend on the beam indices even in the far zone.

B. Circularly polarized wave

We now look at the form of a circularly polarized beam. For a circularly polarized beam of positive helicity we take $f(\vec{r}) = \psi_{mn}(\vec{r})$ and $g(\vec{r}) = i\psi_{mn}(\vec{r})$. Then various fields components are

$$E_1^{(mn)}(\vec{r}) = \frac{A_{mn}}{\sqrt{2}}\psi_{mn}(\vec{r}), \tag{64}$$

$$E_2^{(mn)}(\vec{r}) = i\frac{A_{mn}}{\sqrt{2}}\psi_{mn}(\vec{r}), \tag{65}$$

$$E_3^{(mn)}(\vec{r}) = i\frac{A_{mn}}{2kw_0}[2m\psi_{m-1,n}(\vec{r}) - \psi_{m+1,n}(\vec{r}) + 2in\psi_{m,n-1}(\vec{r}) - i\psi_{m,n+1}(\vec{r})], \tag{66}$$

where A_{mn} is related to the total beam power P_0 by Eq. (39). In the far zone $z \gg z_0$ these equations lead to the following intensity distributions [$I_\perp(\vec{r}) = 2I_1(\vec{r}) = 2I_2(\vec{r})$]:

$$I_\perp(\vec{r}) = \left[\frac{P_0}{2^{m+n}m!n!\pi w^2(z)}\right] H_m^2(X)H_n^2(Y)e^{-(X^2+Y^2)}, \tag{67}$$

$$I_3(\vec{r}) = \frac{1}{(kw_0)^2}(X^2+Y^2)I_\perp(\vec{r}). \tag{68}$$

For a circularly polarized fundamental Gaussian beam with $m = 0 = n$, the intensity distributions are shown in Fig. 5. Note that $I_\perp^{(00)}$ has the form of a Gaussian. The longitudinal component has a circular symmetry about the direction of propagation. In writing down Eqs. (66)–(68) we have dropped some small terms that would predict that a circularly polarized wave of positive helicity has a small admixture of a circularly polarized wave of negative helicity. The intensity of this orthogonal circularly polarized component is again smaller by a factor $1/(kw_0)^4$ compared to the intensity of the dominant circular polarization component. For a circularly polarized TEM_{00} beam, the cross-polarization component once again has four lobes as was the case for a linearly polarized beam. This small component is what will be seen at the output of a crossed circular polarizer.

The fundamental Gaussian beam given by Eqs. (52)–(54) is common to both Hermite-Gaussian and Laguerre-Gaussian sets of modes. The form of the transverse intensity distribution for the fundamental beam remains unchanged during propagation. For all higher order modes, belonging to either the Hermite-Gaussian or the Laguerre-Gaussian family, the intensity distributions change in general as the beams propagate. For completeness we also give the polarization structure of Bessel beams [3]. These beams are said to be nondiffracting in the sense that their transverse field distribution does not depend on z. We consider only the fundamental Bessel beam. The electric field components of such a beam will be given by

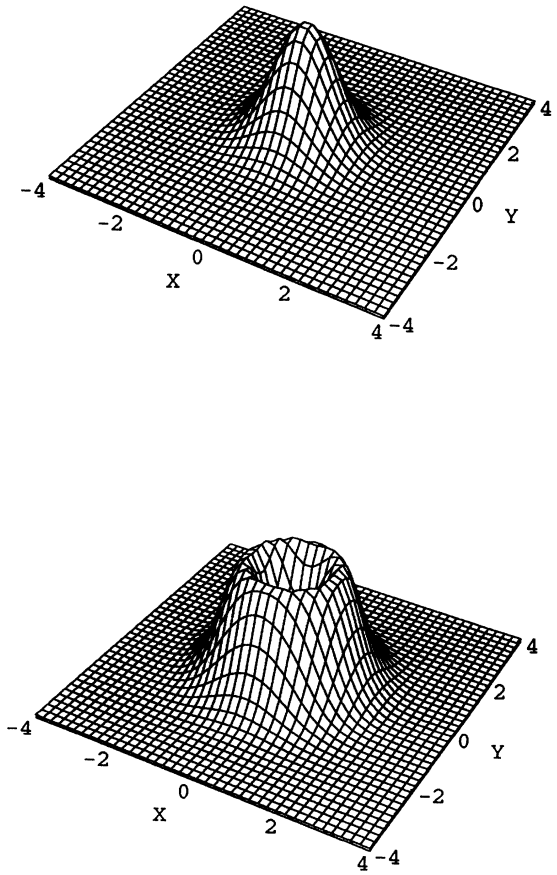

FIG. 5. Intensity profiles for a circularly polarized TEM_{00} wave propagating in the z direction. The profiles are (top to bottom) for the transverse and the longitudinal (z component) field components. $X = \sqrt{2}\,x/w(z)$ and $Y = \sqrt{2}\,y/w(z)$ are the scaled coordinates. Vertical axes in the two profiles are not to scale.

$$E_1(\rho) = AJ_0(\alpha\rho), \tag{69}$$

$$E_2(\rho) = \frac{A\alpha^2 xy}{2k^2\rho^2} J_2(\alpha\rho), \tag{70}$$

$$E_3(\rho) = \frac{-iA\alpha x}{k\rho} J_1(\alpha\rho), \tag{71}$$

where α is determined by the wave frequency ω and propagation constant k via the relation

$$\alpha^2 = (\omega/c)^2 - k^2. \tag{72}$$

Here $J_n(x)$ is the Bessel function of order n and argument x. Since the transverse structure of this beam, given by Eqs. (69)–(71), does not depend on z, it propagates without diffraction. Using Eqs. (69)–(71) in Eq. (43), it can be seen that the Poynting vector for such beams always points in the z direction.

V. EXPERIMENT

Some of the predictions regarding the polarization structure of electromagnetic beams are readily tested with laser beams. Most lasers produce linearly polarized TEM_{00} beams. This is usually due to the presence of polarizing elements such as a Brewster window in the laser cavity. In our experiment, an Ar-ion laser operating at 488 nm was used. The laser had a gain tube with Brewster windows at both ends and operated in the TEM_{00} mode. Light coming out from the Ar-ion laser was passed through a linear polarizer. When the transmission axis of the polarizer coincided with the polarization direction of the incident beam an intense round spot could be seen on a screen. The intensity profile of the laser beam was photographed using a solid state charge coupled device (CCD) camera. A picture of the linearly polarized laser beam was taken with the laser operating at less than 10 mW and the beam attenuated through a neutral density filter (optical density 2). Figure 6 shows the recorded beam profile. It has the general structure corresponding to the distribution (52). When the polarizer is crossed with respect to the direction of polarization of the incident beam four lobes could be seen by the naked eye on a screen placed in a plane transverse to the direction of propagation if the intensity was sufficiently high. Note that according to Eq. (41), the cross-polarization intensity is down by a factor of $1/(kw_0)^2 \sim (\lambda/w_0)^4$ compared to the dominant polarization component. The ratio of the cross-polarization component power to the total beam power, for our laser beam, was $\sim 10^{-11}$ corresponding to the beam waist spot size $w_0 \approx 25\mu$ and wavelength $\lambda = 488$ nm. To observe the cross-polarization component, the laser was operated at 110 mW and the beam was transmitted through a pair of crossed polarizers. The transmission axis of the first polarizer coincided with the polarization direction of the incident light. The intensity of the beam transmitted through the crossed polarizers was recorded, once again, using a CCD camera. Because the polarizers are crossed with respect to the polarization of the incident beam, only the cross-polarization component is transmitted. The bottom row in Fig. 6 shows the cross-polarization intensity distribution. The four-lobe structure predicted by Eq. (53) is clearly seen. It was not possible to get absolute intensity measurements since the polarizers were found to have intensity dependent absorption. This same effect was also observable with unaided eye using an Ar-ion pumped rhodamine-6G dye laser with only about 20–30 mW of yellow orange power due to the increased sensitivity of the eye at these wavelengths. Thus the experiments provide clear evidence

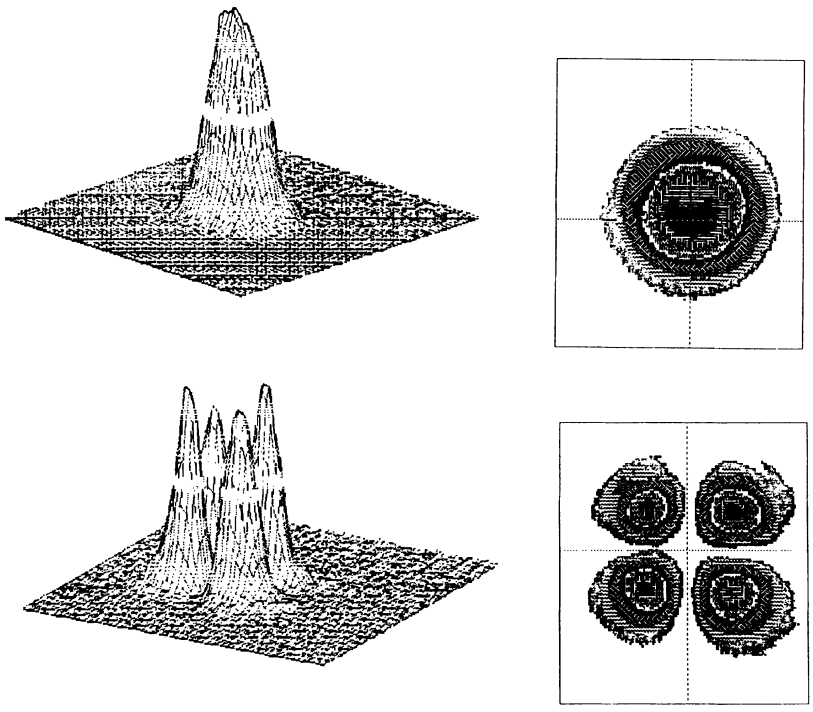

FIG. 6. Experimentally measured beam profiles for a linearly polarized Gaussian TEM_{00} wave. The top row shows the transverse intensity profile (perspective and contour plots) for the dominant polarization component. The bottom row shows the measured intensity profile (perspective and contour plots) for the cross-polarization component after the beam has passed through a pair of crossed polarizers.

for the polarization structure of Hermite-Gaussian laser beams.

In conclusion, we have discussed the polarization and focusing properties of paraxial laser beams. In particular, we have shown that a laser beam of finite transverse cross section with dominant polarization in the x direction has a small longitudinal component and a small cross polarization component in the y direction. The amplitudes of the longitudinal and the cross-polarization field components are smaller by factors λ/w_0 and $(\lambda/w_0)^2$, respectively, compared to the amplitude of the dominant polarization component. Because laser beams have finite transverse extent (λ/w_0 finite) both the cross-polarization and the longitudinal field components must be kept for consistency with Maxwell's equations. The longitudinal component is required for a correct description of the focusing properties of laser beams and the cross-polarization component is required for a correct description of the polarization properties of laser beams. Explicit expressions for the field components of a Hermite-Gaussian laser beam are given. From these considerations it is clear that a pure transverse linearly polarized electromagnetic beam is the geometrical optics limit ($kw_0 \to \infty$) of Eqs. (36)–(38). In general, for a correct description of focusing and polarization properties of laser beams both the longitudinal and the cross-polarization field components must be kept.

ACKNOWLEDGMENTS

Stimulating discussions with the members of the Arkansas Quantum Optics group on this topic are delightfully acknowledged. This work was supported in part by the National Science Foundation.

[1] H. Kogelnik and T. Li, Appl. Opt. **5**, 1150 (1966).
[2] A.E. Siegman, *Lasers* (University Science Books, Mill Valley, CA, 1986), Chap. 16
[3] P.W. Milonni and J.H. Eberly, *Lasers* (Wiley Interscience, New York, 1988), Chap. 14.
[4] J.D. Jackson, *Classical Electrodynamics* (Wiley, New York, 1975), Chap. 7.
[5] M. Lax, W.H. Louisell, and W.B. McKnight, Phys. Rev. A **11**, 1365 (1975).
[6] Y. Fainman and J. Shamir, Appl. Opt. **23**, 3188 (1984).
[7] R. Simon, E.C.G. Sudarshan, and N. Mukunda, Appl. Opt. **26**, 1589 (1987); J. Opt. Soc. Am. A **3**, 536 (1986).
[8] J.P. Barton, D.R. Alexander, and S.A. Schaub, J. Appl. Phys. **64**, 1632 (1988); **65**, 2900 (1989); J.P. Barton and D.R. Alexander, *ibid* **66**, 2800 (1989).
[9] L.W. Davis, Phys. Rev. A **19**, 1177 (1979).
[10] D.N. Pattanayak and G.P. Agrawal, Phys. Rev. A **22**, 1159 (1980).
[11] A first account of the results of this paper was presented at the Optical Society of America Annual Meeting [W.L. Erikson and Surendra Singh, in *OSA Annual Meeting Technical Digest, 1992* (Optical Society of America, Washington, D.C., 1992), Vol. 23, p. 98].
[12] N. N. Lebedev, *Special Functions and Their Applications*, translated by R. A. Silverman (Dover, New York, 1972), Chap. 4.